Hindawi Publishing Corporation
Journal of Nanomaterials
Volume 2014, Article ID 261395, 10 pages
http://dx.doi.org/10.1155/2014/261395

Research Article

Decolorization of Methylene Blue by Ag/$SrSnO_3$ Composites under Ultraviolet Radiation

Patcharanan Junploy,[1] Titipun Thongtem,[1] Somchai Thongtem,[2,3] and Anukorn Phuruangrat[4]

[1] *Department of Chemistry, Faculty of Science, Chiang Mai University, Chiang Mai 50200, Thailand*
[2] *Department of Physics and Materials Science, Faculty of Science, Chiang Mai University, Chiang Mai 50200, Thailand*
[3] *Materials Science Research Center, Faculty of Science, Chiang Mai University, Chiang Mai 50200, Thailand*
[4] *Department of Materials Science and Technology, Faculty of Science, Prince of Songkla University, Hat Yai, Songkhla 90112, Thailand*

Correspondence should be addressed to Titipun Thongtem; ttpthongtem@yahoo.com
and Somchai Thongtem; schthongtem@yahoo.com

Received 22 January 2014; Revised 23 May 2014; Accepted 25 May 2014; Published 3 July 2014

Academic Editor: Tianxi Liu

$SrSn(OH)_6$ precursors synthesized by a cyclic microwave radiation (CMR) process were calcined at 900°C for 3 h to form rod-like $SrSnO_3$. Further, the rod-like $SrSnO_3$ and $AgNO_3$ in ethylene glycol (EG) were ultrasonically vibrated to form rod-like Ag/$SrSnO_3$ composites, characterized by X-ray diffraction (XRD), X-ray photoelectron spectroscopy (XPS), electron microscopy (EM), Fourier transform infrared (FTIR) spectroscopy, and UV-visible analysis. The photocatalyses of rod-like $SrSnO_3$, 1 wt%, 5 wt%, and 10 wt% Ag/$SrSnO_3$ composites were studied for degradation of methylene blue (MB, $C_{16}H_{18}N_3SCl$) dye under ultraviolet (UV) radiation. In this research, the 5 wt% Ag/$SrSnO_3$ composites showed the highest activity, enhanced by the electron-hole separation process. The photoactivity became lower by the excessive Ag nanoparticles due to the negative effect caused by reduction in the absorption of UV radiation.

1. Introduction

Strontium stannate ($SrSnO_3$) is a type of ABO_3 perovskite, at which A is commonly an alkaline earth such as Ca, Sr, and Ba, and B is a p-block posttransition metal in the periodic table. ABO_3 perovskite has been used for energy conversion, lithium ion batteries, stable capacitors, oxygen-permeable ceramic membranes, and gas sensors [1–4]. In recent years, $SrSnO_3$ has been widely used in photocatalytic applications [4–6]. Development of semiconductors to enhance photocatalytic activity by being deposited with noble transition metals like Ag, Au, Pt, and Ir has been intensively investigated. The noble metal/semiconducting oxide composites are able to slow down the rate of electron-hole recombination, due to the better charged separation of electrons and holes. The electrons accumulated on the metal and holes remained on the photocatalytic surfaces [7]. Silver nanoparticles exhibit unexpectedly high photocatalytic activities toward different types of reactions compared to the bulk and promote the performance of photocatalysis [8].

$SrSnO_3$ has been synthesized by different methods such as solid state reaction at a temperature above 1,000°C [2], hydrothermal method [3, 4], microemulsion [9], and polymeric precursor method [10]. Recently, microwave radiation has been used for the synthesis of materials, including inorganic complexes, oxides, and sulfides. Microwave radiation has shown very rapid growth in its application to materials science and engineering due to its unique reaction effect, such as rapid volumetric heating and the consequent dramatic increase in reaction rate [11, 12]. Silver nanoparticles can be deposited on substrates by polyol organic agent as a reducing agent in assisting the nucleation and growth of nanoparticles

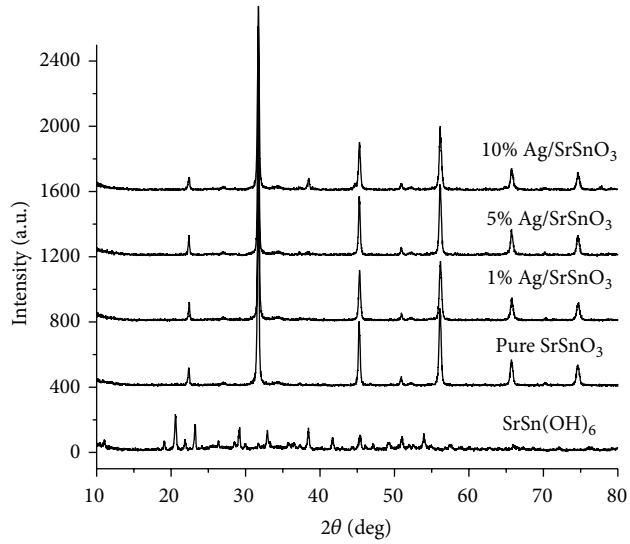

FIGURE 1: XRD patterns of $SrSn(OH)_6$ precursors, pure $SrSnO_3$, 1 wt%, 5 wt%, and 10 wt% $Ag/SrSnO_3$ composites.

on a variety of substrates including silicon/carbon composite microspheres, polymer nanofibers, and TiO_2 nanoparticles [13–15].

In the present research, a cyclic microwave radiation (CMR) used for the synthesis of rod-like $SrSn(OH)_6$ precursors in surfactant-free solution with fast reaction time is reported. Metallic silver nanoparticles were doped with $SrSnO_3$ products to form $Ag/SrSnO_3$ composites, which are new candidates for photocatalysis for waste water treatment.

2. Experimental Procedures

To synthesize $SrSn(OH)_6$ precursors, 0.005 mol strontium acetate ($(CH_3CO_2)_2Sr$) and 0.005 mol tin(II) chloride dihydrate ($SnCl_2{\cdot}2H_2O$) were dissolved in 80 mL deionized water with 30 min continuous stirring at room temperature. The pH was adjusted to 12 using 3 M NaOH with continuous stirring for 1 h until white suspension was obtained. The mixture was irradiated by a 180 W cyclic microwave radiation (1 min on for every 1 min interval) for 30 cycles. The white precipitates were synthesized, separated using a filtered paper, rinsed with deionized water for several times and absolute ethanol, and dried in air at 70°C for 24 h. In the end, the $SrSn(OH)_6$ precursors were calcined in ambient atmosphere at 900°C for 3 h to form the $SrSnO_3$ product.

To synthesize $Ag/SrSnO_3$ composites, 1 wt%, 5 wt%, and 10 wt% $AgNO_3$ and 1 g $SrSnO_3$ were dispersed in 50 mL of ethylene glycol (EG, $C_2H_6O_2$) under magnetic stirring. The solutions were ultrasonically vibrated for 15 min to form products which were separated by filtering, washed with absolute ethanol, and dried in air at 70°C for 24 h to form $Ag/SrSnO_3$ composites. The final composites were labeled with 1 wt% $Ag/SrSnO_3$, 5 wt% $Ag/SrSnO_3$, and 10 wt% $Ag/SrSnO_3$.

The final products were characterized by an X-ray diffractometer (XRD, Philips X'Pert MPD) operating at 20 kV, 15 mA with Cu-K_α line ($\lambda = 0.1542$ nm) at a scanning rate of 0.02 deg/s over the 2θ range of 10–80 deg; X-ray photoelectron spectroscopy (XPS, Kratos Axis Ultra DLD) with a monochromatic Al Kα (1486.6 eV) radiation as the excitation source at 15 kV with spectrum calibration using a C1s electron peak at 285.1 eV; a Fourier transform infrared spectrometer (FTIR, Bruker Tensor 27) with KBr as a diluting agent operating in the range of 1000–400 cm^{-1}; a scanning electron microscope (SEM, JEOL JSM-6335F) operating at 15 kV equipped with an Oxford Instruments INCA energy-dispersive X-ray (EDX) analyzer using Si(Li) as a detector; a transmission electron microscope (TEM, JEOL JEM-2010) with a selected area electron diffractometer (SAED) operating at 200 kV; and a UV-visible spectrometer (Lambda 25 Perkin Elmer) using a UV lamp with the resolution of 2.0 nm. Photocatalytic activities of the products were investigated by studying the degradation of methylene blue (MB, $C_{16}H_{18}N_3SCl$) dye in 100 mL 5.0×10^{-6} M MB aqueous solutions by 100 mg photocatalyst each. The solutions were stirred in the dark condition for 1 h to establish an adsorption-desorption equilibrium of MB dye on the catalyst. Then, the solutions were irradiated by two 15 W UV lamps for different lengths of time for further analysis using the UV-visible spectrometer. The decolorization efficiency was calculated by

$$\text{Decolorization efficiency}\,(\%) = \frac{C_o - C}{C_o} \times 100, \quad (1)$$

where C_o and C were the initial and final concentrations of MB, respectively.

3. Results and Discussion

XRD patterns of different products are shown in Figure 1. The precursors were specified as hexagonal $SrSn(OH)_6$ phase of the JCPDS database number 09-0086 [16]. Upon calcination of the precursors at 900°C for 3 h, the products with

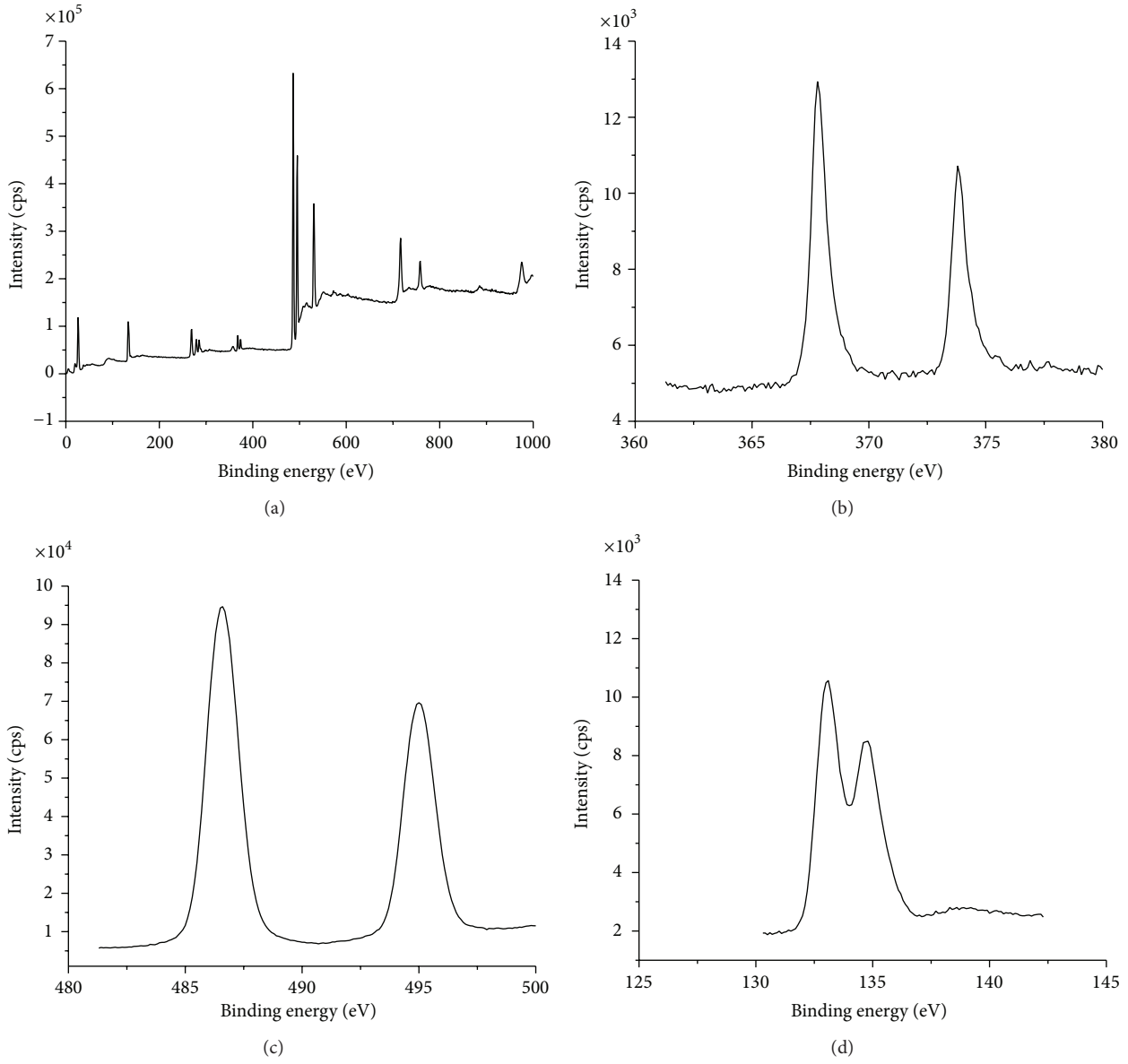

Figure 2: XPS spectra of (a) 10 wt% $Ag/SrSnO_3$, (b) Ag3d, (c) Sn3d, and (d) Sr3d.

high diffraction intensity and better crystalline degree were readily indexed to be orthorhombic perovskite structured $SrSnO_3$ of the JCPDS database number 77-1798 [16]. Then, $SrSnO_3$ products were doped with Ag nanoparticles to form $Ag/SrSnO_3$ composites. Comparing the patterns of the 1 wt% $Ag/SrSnO_3$, 5 wt% $Ag/SrSnO_3$, and 10 wt% $Ag/SrSnO_3$ composites to those of the JCPDS database number 09-0086 [16], they were still being identified as pure orthorhombic $SrSnO_3$ phase. No other peaks were detected in the XRD patterns of 1 wt% and 5 wt% $Ag/SrSnO_3$ composites. Possibly, concentration of Ag was too low to be detected. In case of 10 wt% $Ag/SrSnO_3$ composites, additional two peaks at 2θ of 38.50 and 77.84 deg were detected and specified as the (111) and (311) peaks of cubic Ag of the JCPDS database number 02-1098 [16], due to the reduction process $Ag^+ \rightarrow Ag^0$ by EG during ultrasonic vibration process. This detection indicated that Ag nanoparticles were only deposited on the $SrSnO_3$ surface. The average Ag particle size was estimated by Debye-Scherrer formula

$$D = \frac{0.9\lambda}{\beta \cos\theta}, \tag{2}$$

where λ is wave length of X-ray (0.15418 nm for Cu K_α), β is full width at half maximum (FWHM) in radian, θ is the diffraction angle, and D is particle diameter size [17]. The average particle size is 28.5 nm.

The 10 wt% $Ag/SrSnO_3$ composites were analyzed by XPS to identify the metallic state of silver (Ag^0) on the surface of the composites, as shown in Figure 2. The XPS analysis reveals the existing peaks of strontium, carbon (tape), silver,

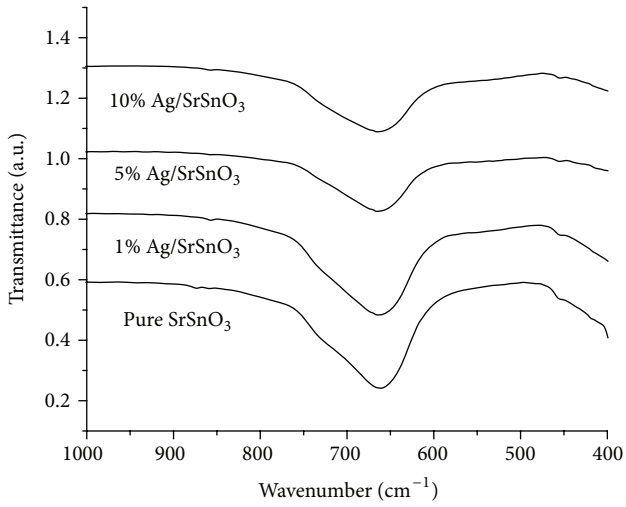

FIGURE 3: FTIR spectra of pure $SrSnO_3$, 1 wt%, 5 wt%, and 10 wt% $Ag/SrSnO_3$ composites.

tin, and oxygen, consistent with the chemical components of the $Ag/SrSnO_3$ composites. The binding energy of C1s line (285.1 eV) was used to calibrate all the binding energies. The analysis reveals the silver 3d spectral lines of spin-orbit doublet peaks with a splitting of 6.07 eV at the binding energy of 367.77 and 373.84 eV for $Ag3d_{5/2}$ and $Ag3d_{3/2}$, respectively. These binding energies correspond with those of the metallic silver of the previous reports [18–21], indicating the presence of Ag^0 in $SrSnO_3$ matrix. The Sn3d peaks of 10 wt% $Ag/SrSnO_3$ composites appear at 486.60 eV of $Sn3d_{5/2}$ and 494.98 eV of $Sn3d_{3/2}$, corresponding to Sn^{4+} [22]. The Sr3d spectrum with spin-orbit doublet peaks corresponds to $Sr3d_{5/2}$ and $Sr3d_{3/2}$ peaks at 133.04 and 134.74 eV, respectively. They are in accordance with Sr^{2+} [23].

The as-synthesized pure $SrSnO_3$ and 1 wt%, 5 wt%, and 10 wt% $Ag/SrSnO_3$ composites were analyzed by FTIR at room temperature over the range from 400 to 1000 cm^{-1} (Figure 3). The vibration of the SnO_3^{2-} stannate groups of pure $SrSnO_3$ was detected as high intensity band at 677 cm^{-1} [24]. Moreover, the bands became shallower with increase in the amount of Ag contained in the $Ag/SrSnO_3$ composites, which indicates the interaction between silver and oxygen atoms in the stannate group of $SrSnO_3$. The result proved that Ag nanoparticles were attached to the surface of $SrSnO_3$ samples.

The products were analyzed by electron microscopy (EM), energy dispersive X-ray (EDX) spectroscopy, and selected area electron diffraction (SAED), as shown in Figures 4, 5, 6, and 7. The $SrSn(OH)_6$ precursors demonstrate the formation of rod-like product with the size distribution of about 300–745 nm in diameter and one to several microns in length. For pure $SrSnO_3$, it still retains the morphology as the $SrSn(OH)_6$ precursors, but the rods became thinner with smooth surface due to the loss of hydroxyl group of the rod-like $SrSn(OH)_6$ precursors by transforming into rod-like $SrSnO_3$. The 10 wt% $Ag/SrSnO_3$ composites remained at the same size and shape as pure $SrSnO_3$ with the aggregated Ag nanoparticles (about 30 nm) formed on the surfaces of $SrSnO_3$ rods. The EDX qualitative analyses of 10 wt% $Ag/SrSnO_3$ composites were recorded as the mapping images of Ag, Sr, Sn, and O, which show the distributive Ag nanoparticles over the $SrSnO_3$ matrix. The EDX spectrum also corresponds to the four prominent peaks belonging to the Sr-L_α, Sn-L_α, O-$K_{\alpha 1,2}$, and Ag-L_α lines without any impurity detection. A SAED pattern shows diffraction rings of the polycrystalline rod-like $SrSn(OH)_6$ precursors corresponding to the (301), (222), (512), and (441) crystallographic planes of the JCPDS database number 09-0086 [16]. SAED patterns of two single crystalline rods of pure $SrSnO_3$ and 10 wt% $Ag/SrSnO_3$ composites were indexed and specified as $SrSnO_3$ orthorhombic phase of the JCPDS database number 77-1798 [16] in accordance with the patterns obtained by simulation. It should be noted that Ag nanoparticles were not detected in the 10 wt% $Ag/SrSnO_3$ composites because the SAED interpretation was selected for characterization only on a very small area.

Figure 8 presents the UV-visible absorption spectra of pure $SrSnO_3$ and 1 wt%, 5 wt%, and 10 wt% $Ag/SrSnO_3$ composites. In this research, the absorption intensity increased significantly around 300 nm in short wavelength for pure $SrSnO_3$ rods, but it did not show the absorption in the visible region, corresponding to the previous reports [4, 24]. By doping with Ag, its absorption intensity on the short-wavelength side was steeply increased compared to that of pure $SrSnO_3$ rods. A small absorption band in the visible region at 437 nm started appearing in the absorption spectrum of the 1 wt% $Ag/SrSnO_3$ composites and gradually shifted to the lower wavelength of 435 nm in the 10 wt% $Ag/SrSnO_3$ composites. Detection of the absorption spectra in the visible light region for $Ag/SrSnO_3$ composites indicates an increase in the absorption intensity with an increase in the Ag content. It is well known that surface plasmon bands appearing in the visible region are characteristic of the noble metal nanoparticles with sizes ranging from 2 nm to 100 nm [25] and surface plasmons are collective oscillations of free electrons at metallic surface [26]. This absorption band is attributed to the characteristic surface plasmon resonance (SPR) phenomenon of free electron in the conduction bands of Ag nanoparticles. When Ag nanoparticles were irradiated by visible light, a large oscillating electric field originated around the metallic particles [26–30]. Clearly, this result indicates the presence of Ag nanoparticles contained in $SrSnO_3$ matrix synthesized by the ultrasonic vibration.

The degradation of MB dye in aqueous solution containing 5 wt% $Ag/SrSnO_3$ composites (Figure 9) under ultraviolet radiation was studied. The intensity decrease in the characteristic absorption peak of MB dye at 663 nm for different lengths of time clearly shows the efficiency of catalytic activity of the photocatalyst. For the decolorization efficiency of MB (Figure 10), almost no degradation of MB dye was detected in the catalyst-free solution although the exposure time was as long as 320 min. This result indicates that the contribution of self-degradation was negligible. But for the solutions containing pure $SrSnO_3$, 1 wt% $Ag/SrSnO_3$, 5 wt% $Ag/SrSnO_3$, and 10 wt% $Ag/SrSnO_3$ composites, the decolorization efficiencies within 320 min were 84.8, 86.3, 99.5, and 92.6%, respectively.

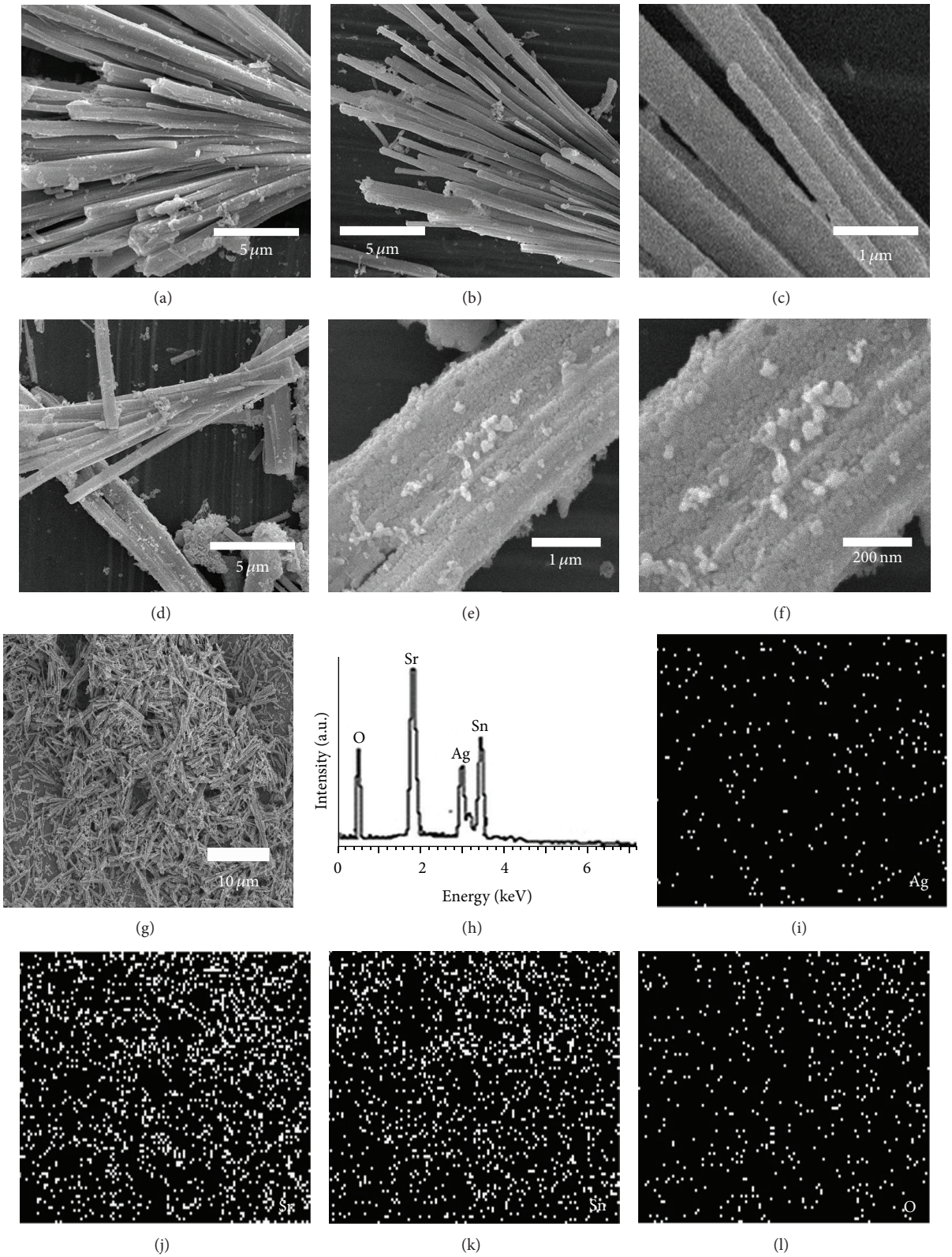

Figure 4: SEM images of (a) $SrSn(OH)_6$ precursors, (b, c) pure $SrSnO_3$, and (d–g) 10 wt% $Ag/SrSnO_3$ composites. (h) EDX spectrum of 10 wt% $Ag/SrSnO_3$ composites and (i–l) EDX mapping for Ag, Sr, Sn, and O of 10 wt% $Ag/SrSnO_3$ composites, respectively.

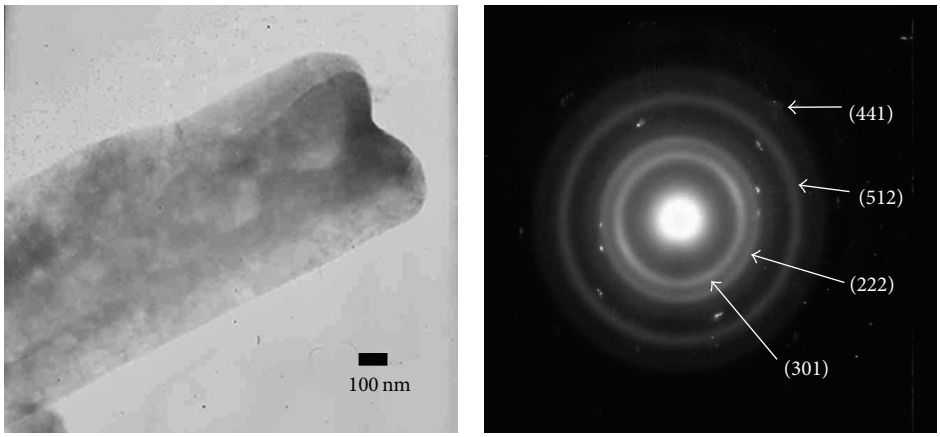

Figure 5: TEM image and SAED pattern of $SrSn(OH)_6$ precursors.

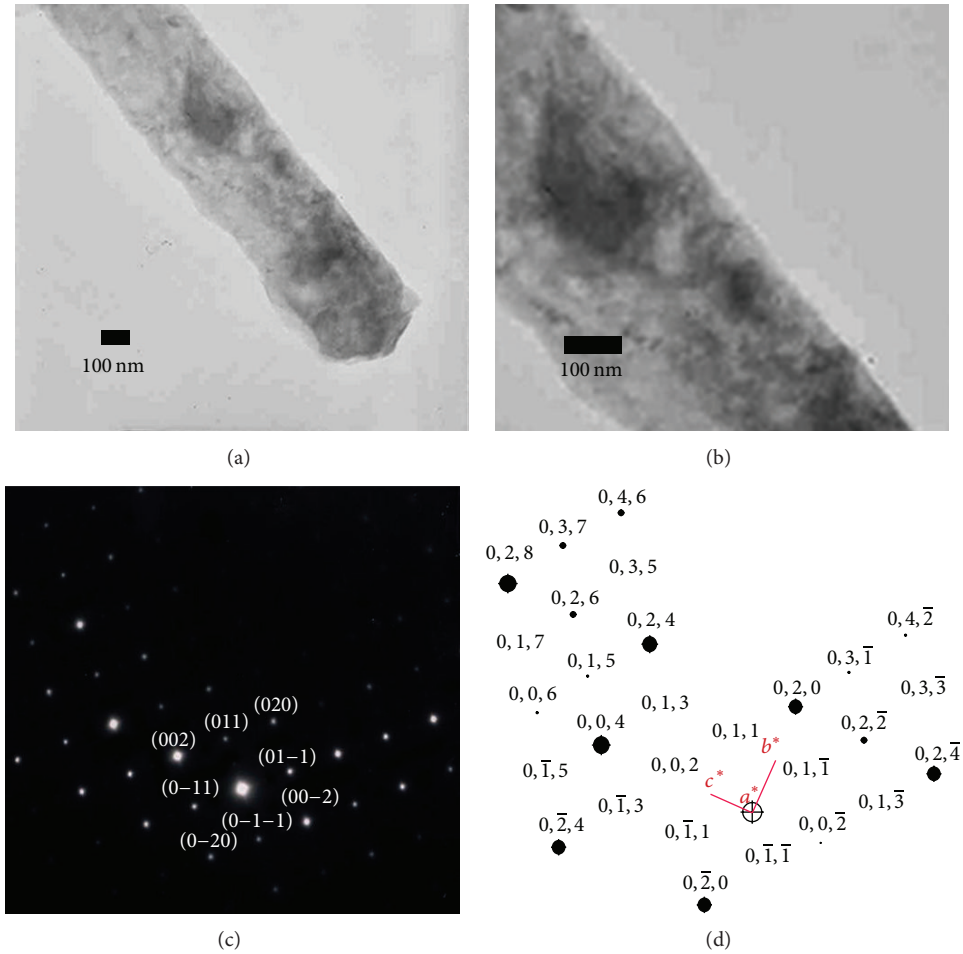

Figure 6: (a, b) TEM images and (c, d) SAED and simulated patterns of pure $SrSnO_3$, respectively.

These implied that 5 wt% $Ag/SrSnO_3$ composites were the best photocatalyst for waste water treatment. The excess of Ag nanoparticles can cause deficiency in the photocatalytic activity of 10 wt% $Ag/SrSnO_3$ composites by lowering the absorption of UV light, leading to the decrease in UV light utilization with negative effect to the photocatalytic process [31]. Moreover, the 5 wt% $Ag/SrSnO_3$ composites were recycled and reused five times to test the photocatalytic stability

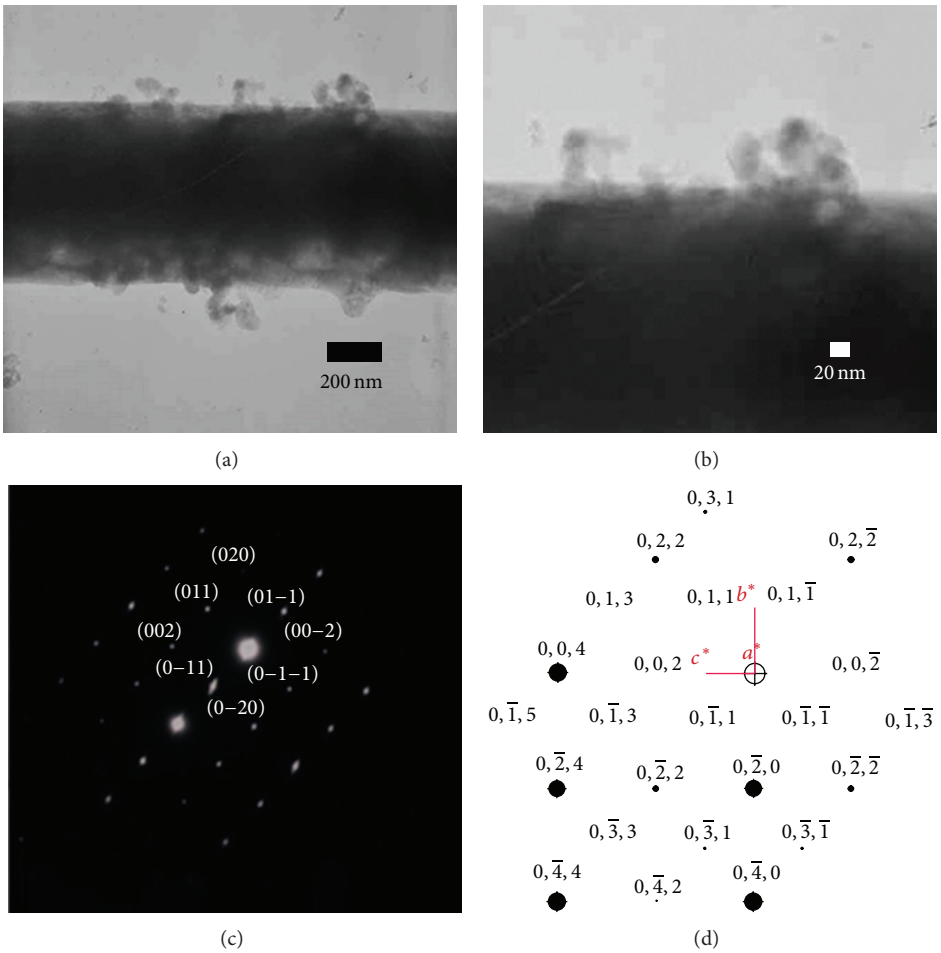

Figure 7: (a, b) TEM images and (c, d) SAED and simulated patterns of 10 wt% Ag/$SrSnO_3$ composites, respectively.

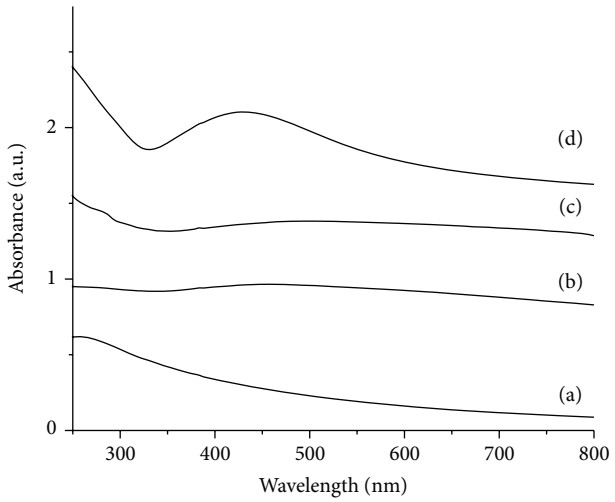

Figure 8: UV-visible absorption of (a) pure $SrSnO_3$ and (b–d) 1 wt%, 5 wt%, and 10 wt% Ag/$SrSnO_3$ composites, respectively.

shown in Figure 11. The photocatalyst is still performing the decolorization efficiency at almost the same rate.

The photocatalysis for organic compounds decomposed by $SrSnO_3$ with and without Ag nanoparticles doping under ultraviolet radiation is proposed (Figure 12). For $SrSnO_3$, electrons in valence band (VB) were excited and transferred to conduction band (CB) under UV light radiation. Then, the photogenerated holes in VB combined with hydroxyl anions to form $^{\bullet}OH$ oxidative species which would further decompose the organic compounds. The rapid recombination rate of electron-hole pairs can lead to low photocatalytic activity. When Ag nanoparticles were added to the $SrSnO_3$ product, the Ag nanoparticles acted as electron traps, inhibiting the electron-hole recombination process. Subsequently, the trapped electrons were transferred to the adsorbed O_2, which acted as electron acceptors. Thus $^{\bullet}O_2^-$ oxidative species were generated and could effectively oxidize the MB dye. Holes still remained in the VB of $SrSnO_3$ and combined with H_2O to form H^+ ions and $^{\bullet}OH$ radicals. These oxidative species could effectively break down toxic organic substances back into original chemical forms of CO_2 and H_2O creating a cleaner and safer environment [32]. The recombination of electron-hole pairs was inhibited, and the photochemical reaction for waste water treatment was enhanced [33, 34].

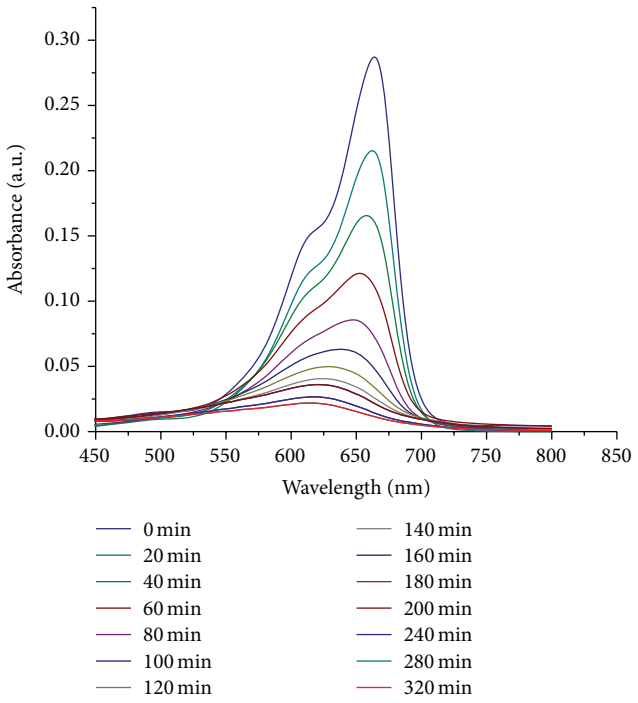

Figure 9: UV-visible absorption of MB photocatalyzed by the 5 wt% $Ag/SrSnO_3$ composites under UV light for different lengths of time.

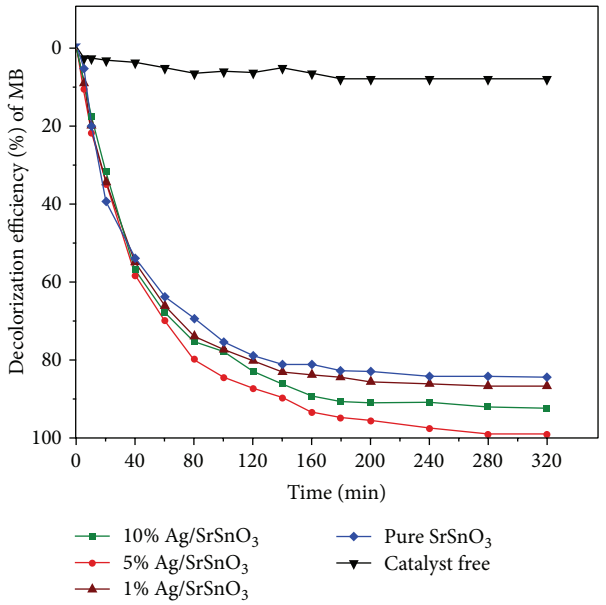

Figure 10: Decolorization efficiencies of MB dye dissolving in different solutions of photocatalyst-free, pure $SrSnO_3$, and 1 wt%, 5 wt%, and 10 wt% $Ag/SrSnO_3$ composites under UV light for different lengths of time.

4. Conclusions

A solution containing strontium acetate and tin(II) chloride dihydrate with the pH of 12 was processed by a cyclic microwave radiation (CMR) to form $SrSn(OH)_6$ precursors, which were calcined at 900°C for 3 h to form $SrSnO_3$. Further, the $SrSnO_3$ precursors and $AgNO_3$ in ethylene glycol were ultrasonically vibrated to form $Ag/SrSnO_3$ composites, which were tested for photocatalysis under ultraviolet radiation for the degradation of MB dye as an organic model. In this research, the 5 wt% $Ag/SrSnO_3$ composites showed the best photocatalyst due to the enhancement of electron-hole separation process.

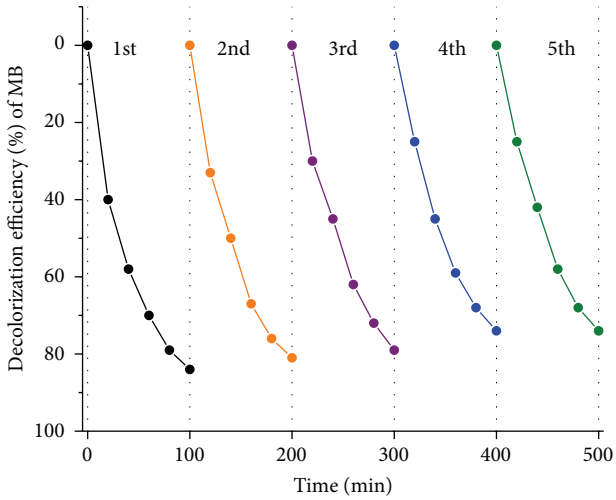

Figure 11: Cycling runs of photodecolorization efficiencies of MB photocatalyzed by 5 wt% $Ag/SrSnO_3$ composites.

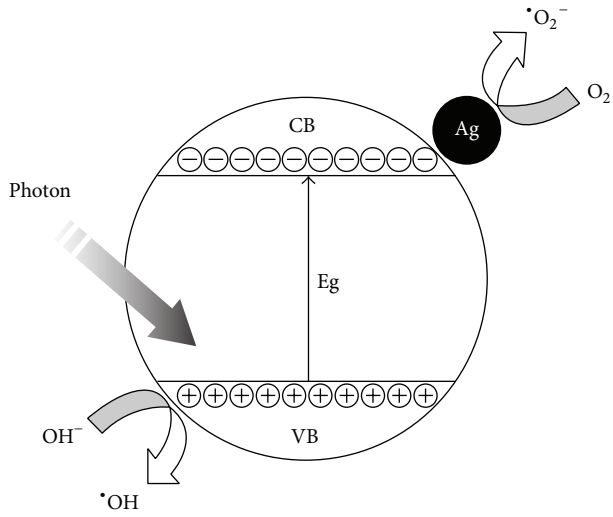

Figure 12: Schematic diagram for the photocatalysis of $Ag/SrSnO_3$ composites.

Conflict of Interests

The authors declare that there is no conflict of interests regarding the publication of this paper.

Acknowledgments

The authors wish to thank the Thailand Research Fund (TRF) for providing financial support through the Royal

Golden Jubilee Ph.D. Program and the TRF Research Grant BRG5380020 and the Thailand's Office of the Higher Education Commission through the National Research University (NRU) Project for Chiang Mai University (CMU), including the Graduate School of CMU through a general support.

References

[1] N. Zidi, S. Omeiri, B. Hadjarab, A. Bouguelia, A. Akroun, and M. Trari, "Transport properties and photo electrochemical characterization of oxygen-deficient $ASnO_{3-\delta}$ (A=Ca, Sr and Ba)," *Physica B*, vol. 405, no. 16, pp. 3355–3359, 2010.

[2] M. C. F. Alves, S. Boursicot, S. Ollivier et al., "Synthesis of $SrSnO_3$ thin films by pulsed laser deposition: Influence of substrate and deposition temperature," *Thin Solid Films*, vol. 519, no. 2, pp. 614–618, 2010.

[3] C. Li, Y. Zhu, S. Fang et al., "Preparation and characterization of $SrSnO_3$ nanorods," *Journal of Physics and Chemistry of Solids*, vol. 72, no. 7, pp. 869–874, 2011.

[4] D. Chen and J. Ye, "$SrSnO_3$ nanostructures: synthesis, characterization, and photocatalytic properties," *Chemistry of Materials*, vol. 19, no. 18, pp. 4585–4591, 2007.

[5] C. W. Lee, D. W. Kim, I. S. Cho et al., "Simple synthesis and characterization of $SrSnO_3$ nanoparticles with enhanced photocatalytic activity," *International Journal of Hydrogen Energy*, vol. 37, no. 14, pp. 10557–10563, 2012.

[6] W. F. Zhang, J. Tang, and J. Ye, "Photoluminescence and photocatalytic properties of $SrSnO_3$ perovskite," *Chemical Physics Letters*, vol. 418, no. 1–3, pp. 174–178, 2006.

[7] H. Sinaim, A. Phuruangrat, S. Thongtem, and T. Thongtem, "Synthesis and characterization of heteronanostructured Ag nanoparticles/MoO_3 nanobelts composites," *Materials Chemistry and Physics*, vol. 132, no. 2-3, pp. 358–363, 2012.

[8] G. Li, K. Chao, C. Ye, and H. Peng, "One-step synthesis of Ag nanoparticles supported on $AgVO_3$ nanobelts," *Materials Letters*, vol. 62, no. 4-5, pp. 735–738, 2008.

[9] J. Ahmed, C. K. Blakely, S. R. Bruno, and V. V. Poltavets, "Synthesis of $MSnO_3$ (M = Ba, Sr) nanoparticles by reverse micelle method and particle size distribution analysis by whole powder pattern modeling," *Materials Research Bulletin*, vol. 47, no. 9, pp. 2282–2287, 2012.

[10] M. C. F. Alves, M. R. Nascimento, S. J. G. Lima et al., "Influence of synthesis conditions on carbonate entrapment in perovskite $SrSnO_3$," *Materials Letters*, vol. 63, no. 1, pp. 118–120, 2009.

[11] T. Ding and J. Zhu, "Microwave heating synthesis of HgS and PbS nanocrystals in ethanol solvent," *Materials Science and Engineering B: Solid-State Materials for Advanced Technology*, vol. 100, no. 3, pp. 307–313, 2003.

[12] T. Thongtem, A. Phuruangrat, and S. Thongtem, "Characterization of nano- and micro-crystalline CdS synthesized using cyclic microwave radiation," *Journal of Physics and Chemistry of Solids*, vol. 69, no. 5-6, pp. 1346–1349, 2008.

[13] E. Kwon, H. S. Lim, Y. K. Sun, and K. D. Suh, "Improved rate capability of lithium-ion batteries with Ag nanoparticles deposited onto silicon/carbon composite microspheres as an anode material," *Solid State Ionics*, vol. 237, pp. 28–33, 2013.

[14] Q. Liu, S. Sun, H. Li et al., "Preparation, characterization and photocatalytic activities of $ZrWMoO_8$/Ag composites with core-shell structure," *Applied Surface Science*, vol. 261, pp. 593–597, 2012.

[15] G. Li, H. Liu, H. Zhao et al., "Chemical assembly of TiO_2 and TiO_2@Ag nanoparticles on silk fiber to produce multifunctional fabrics," *Journal of Colloid and Interface Science*, vol. 358, no. 1, pp. 307–315, 2011.

[16] Powder Diffract File, JCPDS-ICDD, Delaware County, Pa, USA, 2001.

[17] T. Theivasanthi and M. Alagar, "Electrolytic synthesis and characterization of silver nanopowder," *Nano Biomedicine and Engineering*, vol. 4, no. 2, pp. 58–65, 2012.

[18] B. Yu, K. M. Leung, Q. Guo, W. M. Lau, and J. Yang, "Synthesis of Ag-TiO2 composite nano thin film for antimicrobial application," *Nanotechnology*, vol. 22, no. 11, Article ID 115603, 2011.

[19] S. Hu, F. Li, and Z. Fan, "A convenient method to prepare AG deposited N-TiO_2 composite nanoparticles via NH_3 plasma treatment," *Bulletin of the Korean Chemical Society*, vol. 33, no. 7, pp. 2309–2314, 2012.

[20] W. Song, Y. Wang, H. Hu, and B. Zhao, "Fabrication of surface-enhanced Raman scattering-active ZnO/Ag composite microspheres," *Journal of Raman Spectroscopy*, vol. 38, no. 10, pp. 1320–1325, 2007.

[21] X. Zhu, Z. Zhang, K. Wang et al., "A facile route to mechanically durable responsive surfaces with reversible wettability switching," *New Journal of Chemistry*, vol. 36, no. 5, pp. 1280–1284, 2012.

[22] M. Kwoka, L. Ottaviano, M. Passacantando, S. Santucci, G. Czempik, and J. Szuber, "XPS study of the surface chemistry of L-CVD SnO_2 thin films after oxidation," *Thin Solid Films*, vol. 490, no. 1, pp. 36–42, 2005.

[23] V. Kozhukharov, M. Machkova, P. Ivanov, H. J. M. Bouwmeester, and R. van Doorn, "Surface analysis of doped lanthanide cobalt perovskites by X-ray photoelectron spectroscopy," *Journal of Materials Science Letters*, vol. 15, no. 19, pp. 1727–1729, 1996.

[24] P. Junploy, S. Thongtem, and T. Thongtem, "Photoabsorption and photocatalysis of $SrSnO_3$ produced by a cyclic microwave radiation," *Superlattices and Microstructures*, vol. 57, pp. 1–10, 2013.

[25] K. Mollazadeh-Moghaddam, B. V. Moradi, R. Dolatabadi-Bazaz, M. Shakibae, and A. R. Shahverdi, "An enhancing effect of gold nanoparticles on the lethal action of 2450 MHz electromagnetic radiation in microwave oven," *Avicenna Journal of Medical Biotechnology*, vol. 3, no. 4, pp. 195–200, 2011.

[26] S. S. Gasaymeh, S. Radiman, L. Y. Heng, E. Saion, and G. H. M. Saeed, "Synthesis and characterization of silver/polyvinilpirrolidone (Ag/PVP) nanoparticles using gamma irradiation techniques," *African Physical Review*, vol. 4, pp. 31–41, 2010.

[27] L. S. Daniel, H. Nagai, and M. Sato, "Absorption spectra and photocurrent densities of Ag nanoparticle/TiO_2 composite thin films with various amounts of Ag," *Journal of Materials Science*, vol. 48, no. 20, pp. 7162–7170, 2013.

[28] X. Yin, W. Que, D. Fei, F. Shen, and Q. Guo, "Ag nanoparticle/ZnO nanorods nanocomposites derived by a seed-mediated method and their photocatalytic properties," *Journal of Alloys and Compounds*, vol. 524, pp. 13–21, 2012.

[29] R. Chahal, S. Mahendia, A. K. Tomar, and S. Kumar, "Effect of ultraviolet irradiation on the optical and structural characteristics of in-situ prepared PVP-Ag nanocomposites," *Digest Journal of Nanomaterials and Biostructures*, vol. 6, no. 1, pp. 301–308, 2011.

[30] Q. Wang, S. Wang, W. Hang, and Q. Gong, "Optical resonant absorption and third-order nonlinearity of (Au,Ag)-TiO_2 granular composite films," *Journal of Physics D: Applied Physics*, vol. 38, no. 3, pp. 389–391, 2005.

[31] S. Hu, F. Li, and Z. Fan, "Preparation of SiO_2-coated TiO_2 composite materials with enhanced photocatalytic activity under UV light," *Bulletin of the Korean Chemical Society*, vol. 33, no. 6, pp. 1895–1899, 2012.

[32] C. Wu and J. Chern, "Kinetics of photocatalytic decomposition of methylene blue," *Industrial and Engineering Chemistry Research*, vol. 45, no. 19, pp. 6450–6457, 2006.

[33] C. Yu and J. C. Yu, "Sonochemical fabrication, characterization and photocatalytic properties of Ag/$ZnWO_4$ nanorod catalyst," *Materials Science and Engineering B: Solid-State Materials for Advanced Technology*, vol. 164, no. 1, pp. 16–22, 2009.

[34] C. Gu, C. Cheng, H. Huang, T. Wong, N. Wang, and T. Zhang, "Growth and photocatalytic activity of dendrite-like ZnO@Ag heterostructure nanocrystals," *Crystal Growth & Design*, vol. 9, no. 7, pp. 3278–3285, 2009.